European Journal of Pharmaceutics and Biopharmaceutics 108 (2016) 9–17

Contents lists available at ScienceDirect

European Journal of Pharmaceutics and Biopharmaceutics

journal homepage: www.elsevier.com/locate/ejpb

Research paper

# Dissolution profile of theophylline modified release tablets, using a biorelevant Dynamic Colon Model (DCM)

Konstantinos Stamatopoulos [a,*], Hannah K. Batchelor [b,*], Mark. J.H. Simmons [a]

[a] School of Chemical Engineering, University of Birmingham, Birmingham B15 2TT, United Kingdom
[b] Pharmacy and Therapeutics Section, Institute of Clinical Sciences, College of Medical and Dental Sciences, Medical School Building, University of Birmingham, Edgbaston, Birmingham B15 2TT, United Kingdom

ARTICLE INFO

*Article history:*
Received 26 May 2016
Revised 13 July 2016
Accepted in revised form 8 August 2016
Available online 13 August 2016

*Keywords:*
Theophylline
Biorelevant dissolution test
Extended release tablets
Proximal colon
*In vitro* model

ABSTRACT

The human proximal colon has been considered a favourable site to deliver drugs for local and systemic treatments. However, modified dosage forms face a complex and dynamically changing colonic environment. Therefore, it has been realized that in addition to the use of biorelevant media, the hydrodynamics also need to be reproduced to create a powerful *in vitro* dissolution model to enable *in vivo* performance of the dosage forms to be predicted.

A novel biorelevant Dynamic Colon Model (DCM) has been developed which provides a realistic environment in terms of the architecture of the smooth muscle, the physical pressures and the motility patterns occurring in the proximal human colon. Measurements of pressure inside the DCM tube confirmed a direct association between the magnitude of the pressure signal with the occlusion rate of the membrane and the viscosity of the fluid.

The dissolution profile and the distribution of the highly soluble drug, theophylline, were assessed by collecting samples at different locations along the DCM tube. Differences in the release rates of the drug were observed which were affected by the sampling point location, the viscosity of the fluid and the mixing within the DCM tube. Images of the overall convective motion of the fluid inside the DCM tube obtained using Positron Emission Tomography enabled relation of the distribution of the tracer to likely areas of high and low concentrations of the theophylline drug.

This information provides improved understanding of how extensive phenomena such as supersaturation and precipitation of the drug may be during the passage of the dosage form through the proximal colon.



## 1. Introduction

The environment of the human colon is considered favourable for systemic and local delivery of drugs [1,2]. The neutral pH, the reduced digestive enzymatic activity, the higher responsiveness to absorption enhancers (e.g. chitosan) [3] and the much longer transit times compared to the upper gastrointestinal (GI) tract [4], make the colon an attractive site for drug delivery.

Predictive dissolution methods can contribute to a reduction in or refinement of *in vivo* studies during the design, development and evaluation of drug delivery systems. Thus, the establishment of an *in vivo-in vitro* correlation is of great importance. Temperature, pH, ionic strength, buffer capacity, presence of surfactants and/or digestive enzymes, greatly influence the release of the drug from modified-release dosage forms [5]. However, it has been realized that both physicochemical characteristics of the gastrointestinal fluids as well as hydrodynamics need to be reproduced in order to make a powerful *in vitro* model to predict *in vivo* performance [5–7]. Existing compendial dissolution methods oversimplify the complex and dynamic environment of the human colon [8]. Thus, apart from the application of the biorelevant media in the dissolution methods [9–13], attempts have been made to improve the bio-relevance of the hydrodynamic and mechanical conditions in dissolution methods [5,14–17].

A physiologically realistic engineering intestinal model needs to be able to reproduce the widely accepted law of the intestine [18], which states that the colonic fluids move in the digestive tract due to the combined ascending excitatory (muscle contraction)

* Corresponding authors at: School of Chemical Engineering, The University of Birmingham, Edgbaston, B15 2TT Birmingham, United Kingdom (K. Stamatopoulos). School of Pharmacy, University of Birmingham, Edgbaston, B15 2TT, United Kingdom (H.K. Batchelor).

*E-mail addresses:* KXS231@bham.ac.uk (K. Stamatopoulos), h.k.batchelor@bham.ac.uk (H.K. Batchelor).

http://dx.doi.org/10.1016/j.ejpb.2016.08.004
0939-6411/

coupled with the forward descending inhibition (muscle relaxation) [19]. Furthermore, the structure and the activity of the smooth muscle act to regulate the mixing, transport and the residence times of the colonic fluids [20,21]. In particular, the presence of taeniae (the thick layer of the longitudinal muscle) and semilunar folds, which form the characteristic pockets in the colon which are termed the haustra, seems to play a major role in the regulation of colonic fluid transit through the colon [21].

Advances in manometry [22] and in non-invasive monitoring systems [23,24] have provided insights on colon motility and transit times; demonstrating the complex and dynamic environment that a modified dosage form is exposed to during its passage through the lower GI tract. Five types of propagating motor patterns have been identified by use of high – resolution fibre – optic manometry [22]. Four of them (cyclic motor, short single, long single and occasional retrograde motor pattern) are related to low – amplitude propagating sequences (range of average values: 2–10 mmHg) and form the majority of the motility events [22]. The remaining pattern forms high – amplitude propagating sequences (PSs) (>116 mmHg) [22]. The low – amplitude PSs were as likely to be associated with colonic movements as high - amplitude PSs [25]. However, the low – amplitude PSs seem to be related mainly to the mixing of fluids (segmentation) [26] whereas high – amplitude PSs cause mass movements (peristalsis) of the colonic fluids [27]. However, the pressure signal of the catheter is affected by the viscosity of the colonic fluids [28]. Arkwright et al. [28] showed that the predetermined amplitude of the applied pressure on a flexible wall was not the same as the pressure measured by the catheter placed inside the elastic tube filled with viscous lumen. Thus, *in vitro* models should take this into consideration. Otherwise, it is likely that the applied pressures in the lumen by the flexible tube, like in case of the large intestine simulator TIM-2 [29], will not accurately reflect the physical amplitudes.

*In vivo* studies of the human colon have shown that other factors, in addition to the PSs, affect the propulsion and the mixing of the colonic fluids [25]. The travel distance of the PSs, the viscosity [30] and the reflux of 50% of the bolus, slow the propulsion of the fluids [25]. Thus, the mixing of the colonic fluids is served with the combination of these parameters causing 'to and fro' motion of the contents.

Most of drugs have been targeted at the proximal human colon (i.e. caecum and ascending section) because it is a good potential site for absorption with its high water content, larger surface area as well as higher bacterial activity [31]. The volume of the colonic fluids does not differ significantly in fasted and fed state [32] and varies with a range 10–125 mL [33]. However, magnetic resonance imaging studies have shown the fluids are distributed along the colon in the form of pockets [32]; for instance, 13 mL could be distributed among four pockets (i.e. haustra) [33].

It is clear that apart from the use of biorelevant media, the proper simulation of the hydrodynamics in proximal colon should be performed via the reproduction of the architecture of the colon. Moreover, the volume and the spread of the fluids will also affect the dissolution and the distribution of the drug along the proximal colon. The distribution of the drug could be also considered as a parameter which might determine the fraction of the absorptive surface area of the colon wall on which the drug will be exposed. Thus, it is also critical to understand how colon motility influences not only the dissolution profile but also the distribution of the drug within the proximal colon.

The aim of this study was to develop a computer – controlled Dynamic Colon Model (DCM), in order to understand the colonic behaviour of an extended release oral dosage form exposed to a more realistic colonic environment. Specifically the model was designed to reproduce the anatomy and propagating motor patterns within the human proximal colon. A solid phase catheter was used to monitor the pressure forces generated by the wall motion within the DCM and Positron Emission Tomography (PET) was used to visualize the overall convection of fluids. The dissolution behaviour of an extended release dosage form (theophylline) was assessed in different viscous media within the DCM; the different media represented the dewatering process which takes place in the human colon.

## 2. Materials and methods

### 2.1. Materials

Sodium carboxymethylcellulose (NaCMC) of 90,000 and 700,000 molecular weight was purchased from Sigma (St., Louis, USA). Theophylline anhydrous and potato starch were bought from Acros Organics (Loughborough, UK). Sodium hydroxide, hydrochloric acid (1 M), potassium hydrogen ($KH_2PO_4$) and dihydrogen phosphate ($K_2HPO_4$) were purchased from Sigma (St., Louis, USA). The radioactive solution of radionuclide $^{18}F$, used in PET experiments, was provided from the School of Physics and Astronomy of the University of Birmingham, UK.

### 2.2. Manometric measurements

A solid state catheter manufactured by Unisensor (Unisensor AG, Attikon, CH-8544, Switzerland) was used for the experimental studies. The catheter was 2.6 mm in diameter and contained 1 pressure sensing element. The calibration of the pressure sensor was performed by placing the catheter in a tube filled with distilled water. The system was well sealed with no air or water leakage. Then, using a hand pump manometer, predetermined pressure intervals were applied within the range of 0–300 mmHg and the voltage output of the catheter was recorded. In order to measure local pressure events generated by the oscillation of a single unit of the DCM tube a modified version of the apparatus used by Arkwright et al. [28] was developed (supplementary material). Since the interpretation of the manometric data is affected by the viscosity of the fluids [28], the signal output of the catheter was recorded in different solutions of NaCMC (0.25, 0.50 and 0.75%, (w/w)) for fixed membrane occlusion degree (73%; avoiding physical contact with the catheter) and occlusion rates of 4.3 mm $s^{-1}$, 8.5 mm $s^{-1}$ and 16.6 mm $s^{-1}$.

### 2.3. Dynamic Colon Model (DCM)

A schematic representation of the novel DCM tube is presented in Fig. 1. The tube consists of ten segments with 20 cm total length and diameter 5 cm, to match the average values that typically seen in the human proximal colon [34]. Inflation and deflation of the membrane of each segment is controlled by a hydraulic system producing an antegrade (forward) wave at a speed of 2 cm $s^{-1}$ which is representative of the human colon [22,25].

Fig. 2a shows the membrane's displacement profile of each individual segment and the overall profile of the propagating wall motion (Fig. 2b). In order to reproduce the intestine law (i.e. contraction of the first segment with the simultaneous relaxation of the proximal segment), the profile of the wave of the DCM wall was set up as follows: (1) the membrane of the first segment was inflated whereas in the second it was deflated at the same speed 1.6 cm $s^{-1}$; (2) When the first segment reaches the maximum occlusion degree (i.e. 73%), it stays at this position for 1 s before going back to its neutral position with a speed of 0.35 cm $s^{-1}$. The slower speed was used in order to mimic the relaxation of the colon wall. In addition, keeping the segment at the contraction stage for 1 s prevents backflow as shown in

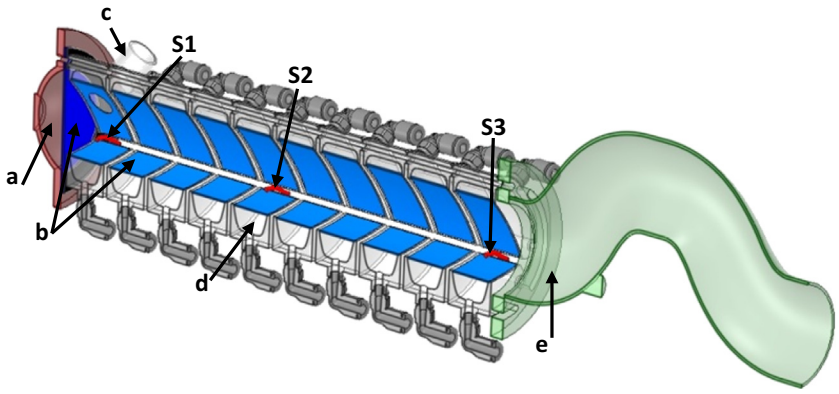


**Fig. 1.** 3D model of DCM tube using ANSYS Spaceclaim 2015. The DCM tube is consisted by: (a) a hemispherical acrylic body which represents the caecum; (b) the flexible membrane; (c) the inlet which represents the ileocolonic junction zone; (d) the triangular configured segment with the characteristic haustrum; (e) a rigid siphon which represents the hepatic flexure; S1, S2 and S3 represent the location of the sampling points along the DCM tube.

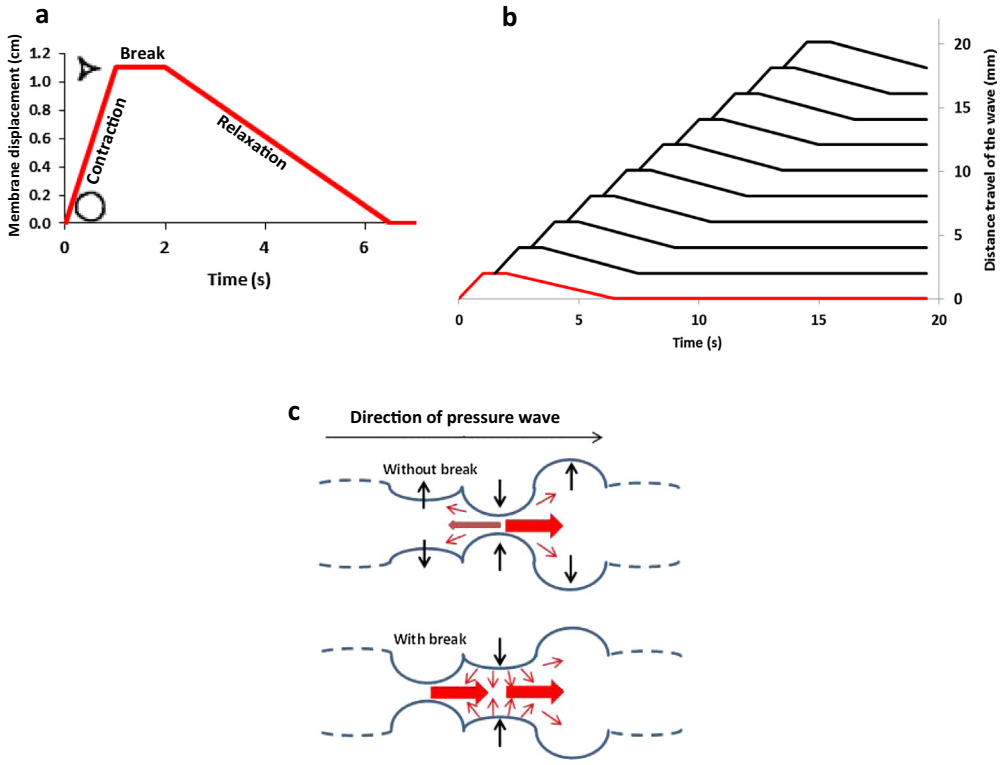


**Fig. 2.** (a) Profile of contraction-break-relaxation cycle of each segment; (b) profile of the travelling peristaltic wave along the artificial colon tube; (c) a forwardly fluid flow is formed by introducing a standing period (break) at the contraction stage of the starting segment.

Fig. 2c. The timings of the motion of each segment were aligned so that the motion within the DCM was representative of that within the human colon and minimized backflow within the DCM.

### 2.4. Dissolution experiments

The dissolution profile of the theophylline released from the NaCMC (90,000) based tablet was assessed in different viscous media and under a fixed motion of DCM flexible wall which was engineered to mimic the main motility pattern observed in human proximal colon. The tablet was directly introduced into the pre-filled DCM tube, assuming that the dosage form reached the human colon intact. This approach is not far from the reality since studies have shown that colon-specific coated formulations reach the lower GI tract intact [35].

$NaCMC_{(90,000)}$ based tablets of 500 mg were prepared for the dissolution experiments. The composition was as follows: 50% (w/w) theophylline, 44% (w/w) $NaCMC_{(90,000)}$, 5% (w/w) potato starch and 1% (w/w) silicone dioxide. The excipients were sieved, mixed manually for 10 min and tableted using a single die tableting machine (Kilian, Coln, D) with a piezoelectric load washer (Kistler, Winterthur, CH) fitted with flat-faced 9.8 mm punch. A load pressure of 1961.2 bar was applied. The cylindrical tablets had a final weight of 500 ± 15 mg.

The dissolution experiments were set up based on two assumptions: (i) the DCM tube was placed horizontally in accordance with the normal reclining position of patients during manometric, scintigraphy and MRI procedures; (ii) it is assumed that the DCM operates in the fed state in which more propagating sequences of pressure waves are taking place in proximal colon [22]. The DCM

tube was filled to 50% full which corresponds to 100 mL of $NaCMC_{(700,000)}$ using solutions with different concentrations (0.25 and 0.50%, w/w). This volume was chosen in order to compare the results with the published data obtained from the mini volume USP 2 [36]. In addition, 100 mL is close to the overall volume that a dosage form is likely to be exposed to during its passage through the human colon [37].

The frequency of the pressure events during the dissolution test was set up to represent values within the human colon previously reported in the literature [25]. Thus, the total duration time of the dissolution experiments was selected to be 560 min and every 5 min an antegrade propagating sequence (APS) was applied. Samples were collected from three different locations: at the beginning (S1), in the middle (S2) and at the end (S3) of the DCM tube in order to evaluate the distribution of the released drug. The samples were collected at predetermined time intervals (5, 10, 30, 60, 120, 240, 360, 480 and 560 min). Subsequently, all the samples were passed through a 0.4 μm PTFE filter [36] prior to the quantitative analysis of theophylline which was performed according to Stamatopoulos et al. [36]. The temperature during the dissolution experiments was maintained at 37 °C using a 300 W infrared ceramic lamp. The volume of the medium removed at each time point was replaced with fresh media.

### 2.5. Positron Emission Tomography (PET) experiments

The Positron Emission Tomography system at the University of Birmingham was used in order to assess the mixing process within the DCM tube under APS waves. Details of the PET system can be found in Broadbent et al. [38]. Fig. 3 illustrates the DCM setup between the two PET cameras and the coordinate system used as a reference. The half-filled DCM tube was placed between the two positron cameras and 1 mL of radiolabelled water was injected in the first segment through a hole of 1 cm ∅, which represents the human ileocolonic junction. Ten antegrade waves, with 10 s time delay between them, were applied. As in scintigraphy studies, each PET image shows the distribution of the radioactive solution along the length of the DCM tube. The PET data were used to correlate to the dissolution data of the theophylline tablets.

## 3. Results and discussion

### 3.1. Determination of the pressures inside a DCM segment using manometry

Manometry is a well-established method for recording the motility events in the lower GI tract as well as diagnosing abnormalities in the human colon [39]. However, manometry measurements are affected by the viscosity of the fluids [28]. Thus, the pressure signal generated from the oscillation of the flexible wall of DCM tube is recorded using fluid of increasing viscosity. Fig. 4 shows the measured pressures obtained with using fluids of different $NaCMC_{(700,000)}$ concentrations. It is clear that as the viscosity is increased the measured pressure signal is also increased. In addition, the solid state catheter used in this study can record non-occluding events (i.e. no physical contact of the membrane with the catheter). This is important when other motility patterns rather than high-amplitude propagating sequences need to be reproduced in *in vitro* models in order to assess the performance of the dosage forms, since the majority of the motility events are of low amplitude [40]. It is noticed that the higher the rate of occlusion, the sharper is the peak of recorded pressure. These observations were in agreement with that described by Arkwright et al. [28]. The measured pressure in water was 1 mmHg regardless of the membrane occlusion rate whereas significant increase in pressure signal was observed from 2.5 to 5 mmHg when the concentration of NaCMC was ⩾0.62% (w/w) and the occlusion rate increased from 4.3 mm $s^{-1}$ to 16.6 mm $s^{-1}$. The measured pressures generated by the wall motion of the DCM tube were within the range of *in vivo* amplitudes recorded with the use of high resolution catheters [22]. Dinning et al. [22], showed that the amplitudes recorded in proximal colon prior to a meal were below 2 mmHg whereas after meal were between 2 and 4 mmHg. However, it is not possible for the authors to know the viscosity of the colonic fluids or the occlusion degree of the colon wall, during the recording time, in order to assess the impact of these two parameters on the interpretation of the manometric measurements. Nevertheless, the viscosity of the colonic fluids is likely to increase during the experimental study (4 h manometric recording time) since the net absorption rate of the water observed in human colon is 2.7 ± 0.3 mL $min^{-1}$ [41]. In addition, high pressure signals of 100 mmHg magnitude were only observed when the membrane touched and partially squeezed the pressure sensor of the solid state catheter used in our study. Thus, apart from the high amplitude propagating sequences, the *in vivo* values recorded in proximal colon [22] might represent mainly non-occluding events under continuously variable viscosity of the colonic fluids. Therefore, the experimental conditions in our study and hence the measured pressures could be considered biorelevant when compared with the available *in vivo* data.

### 3.2. Release profile of theophylline in different viscous media

Fig. 5 shows the dissolution profile of the theophylline in viscous media which was obtained from the three different sampling points, located at the beginning, at the middle and at the end of the DCM tube. The results for the 0.25% $NaCMC_{(700,000)}$ (w/w) solution (Fig. 5a), show that there was an unequal distribution of the

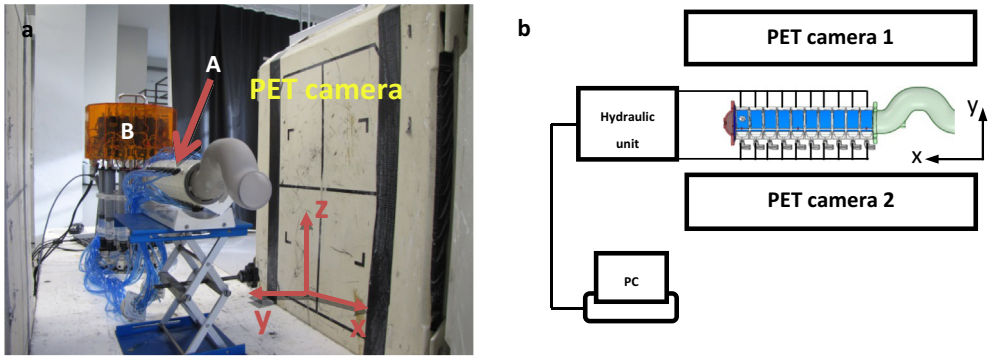


**Fig. 3.** (a) DCM tube (A) in between PET cameras coupled with the hydraulic system (B); (b) schematic representation of the DCM – PET configuration.

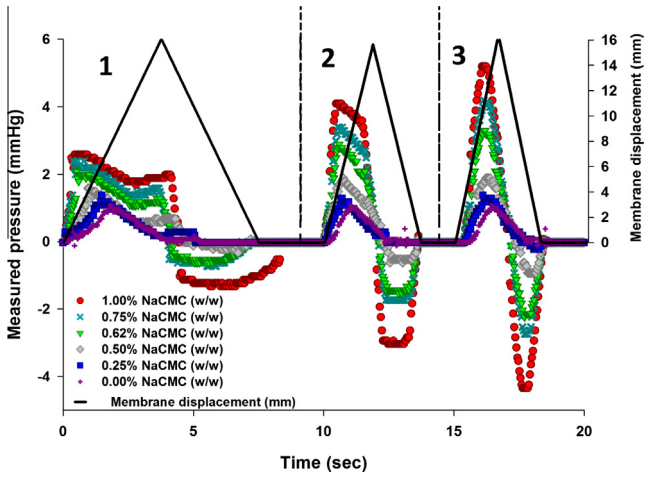


**Fig. 4.** Measure changes in pressure on the lumen for different $NaCMC_{(700,000)}$ concentrations (● 1.00%, × 0.75%, ▼ 0.62%, ◆ 0.50%, ■ 0.25%, + 0.00%, (w/w)) and membrane occlusion rates: (1) 4.3 mm $s^{-1}$; (2) 8.5 mm $s^{-1}$; (3) 16.6 mm $s^{-1}$.

released drug along the length of the tube, resulting in a different release rate. The highest release rate, and hence the highest concentration, was observed at the beginning of the DCM tube, where the tablet was initially located, followed by the second sampling point and finally by the third one located at the end of the tube, as expected. The dissolution profile of the theophylline in 0.50% NaCMC (w/w) (Fig. 5b) followed the same order as in 0.25% NaCMC (w/w) in terms of the release rate according to the sampling point. The results showed relatively similar release rate of the drug in S1 for the 0.50% NaCMC (w/w) to that one in 0.25% NaCMC (w/w) for the same sampling point, but very slow for the other two sampling points (i.e. S2, S3). In particular, at the following sampling time points, i.e. 2, 6 and 8 h, the released drug (%) in 0.25% NaCMC (w/w) was within the range of 3.7%–30.7%, 15%–76.6% and 34.8%–85.5% respectively, whereas in 0.5% NaCMC was 0.2%–29.5%, 0.5%–82.4% and 3%–76.7%. The lower values in all above ranges correspond to S3 and the high ones to S1. These results demonstrated several key features. Firstly, the fluctuations in the drug concentrations and hence of the dissolution profile, most likely reflect the ineffective transport of the drug along the tube, resulting in the formation of areas with high accumulation of the drug; especially at the beginning of the DCM tube, at which the tablet had been introduced. Furthermore, the distribution of the drug in 0.50% NaCMC (w/w) solution was less efficient compared to 0.25% NaCMC (w/w), as anticipated. In the case of 0.50% NaCMC (w/w), most of the drug was accumulated mainly at the beginning of the tube giving release rates close to those obtained in 0.25% NaCMC (w/w). However, this does not mean a faster hydration of the tablet and hence a faster release of the drug in more viscous media [36]. It means that beside the slower release rate of the drug, the inadequate transport in 0.50 NaCMC (w/w) solution leads to high accumulation of the drug molecules in a small area, which may be of value in the local treatment of the ascending colon. In contrast, the distribution of the drug in 0.25% NaCMC (w/w) seems to be more effective.

Second, higher variability was observed in the dissolution data obtained with using 0.50% NaCMC (w/w). It was noticed, by plotting separately the dissolution data of two single different runs, that the dissolution curves of S1 and S2, to a much lesser extent of S3, showed completely different profile (Fig. 6) compared to the dissolution curves of S1 and S2 obtained in the less viscous solution (0.25% NaCMC (w/w)). It seems that except the non-homogeneous distribution of the drug along the DCM tube, the location as well as the erosion of the tablet due to wall motion might affect the release rate of the drug. Indeed, images from the interior of the DCM tube (Fig. 7A) showed fragments of the dosage form which were found to be located either in the cavity of the membrane (Fig. 7B) or on the connection point, the so-called semilunar folds, between the two segments. It seems that if the tablet is located within the cavity of the membrane then the disintegration could be intensive, since the membrane will squeeze and break the dosage form. These observations in combination with the poor distribution of the released drug could explain the differences observed in dissolution profiles and consequently the irregular absorption profiles observed from extended release tablets [5]. Moreover, observations of the final solution of 0.25% NaCMC (w/w) (supplementary material) collected after the end of the dissolution experiments, showed that the dosage form had been disintegrated in small agglomerates.

### 3.3. Visual identification of propagating wall motion of DCM tube using Positron Emission Tomography (PET)

In order to better understand the fluctuations in the concentration of the drug along the tube caused by the wall motion of DCM, PET experiments were performed. This was possible by recording the intensity of the radioactive tracer injected at the beginning of the tube, during repeating APSs waves with 10 s time delay. This time delay was allowed to represent sequential waves whilst condensing the overall time of the experiment to manage the lifespan

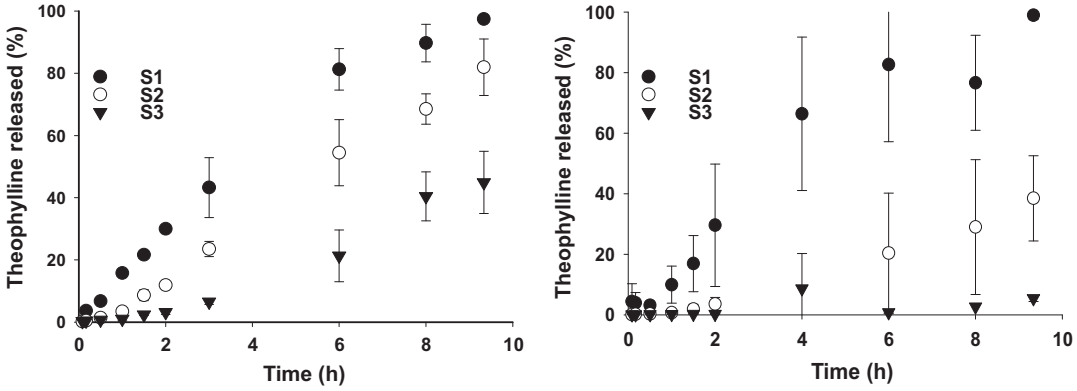


**Fig. 5.** Dissolution curves of theophylline obtained from three different sampling points along the length of the DCM tube (◆ S1; ■ S2; ▲ S3). The dissolution experiments were performed in (a) 0.25% and (b) 0.50% $NaCMC_{(700,000)}$ (w/w) solutions adjusted at pH 7.4 using phosphate buffer; Temperature was 37 °C; Standard deviation bars for the dissolution profile theophylline (n = 6).

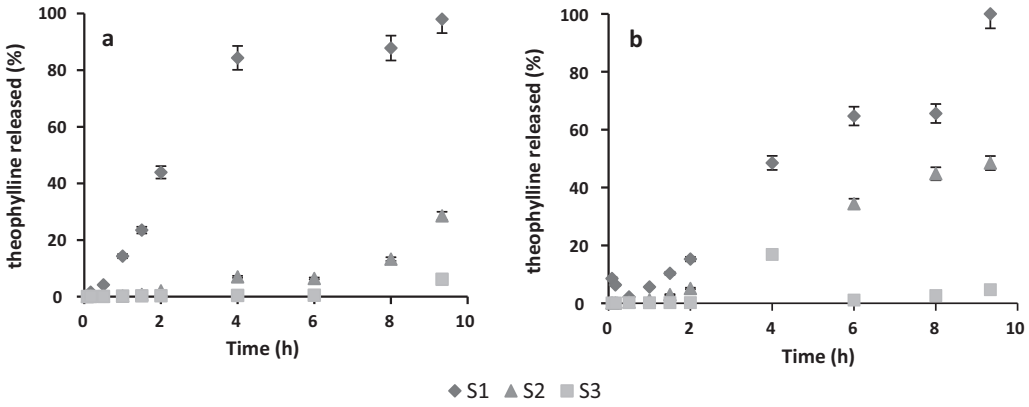


**Fig. 6.** Dissolution profile of theophylline of two different runs in 0.50% NaCMC (w/w) adjusted at pH 7.4 using phosphate buffer. The dissolution curves were obtained from three different sampling points along the length of the DCM tube (◆ S1; ▲ S2; ■ S3). Temperature was 37 °C; Error bars for the dissolution profile of theophylline (n = 3).

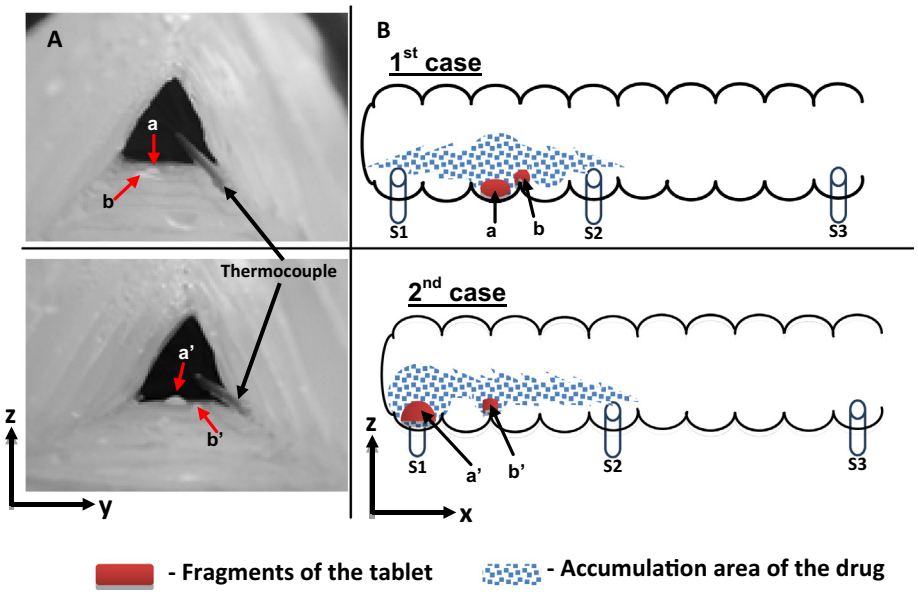


**Fig. 7.** (A) Images of the cross section of the DCM tube and (B) schematic illustration of the *in vitro* model along the x axis, showing the position of the partially disintegrated tablet in two separated runs of the dissolution experiments.

of the radioactive marker. A 10 s delay provided sufficient time for the fluid to become static between waves.

PET images of the 0.25% NaCMC solution (Fig. 8) showed a gradual distribution of the radioactive tracer along the DCM, with only a small amount of tracer detected at the very end of the tube even after 10 waves (Fig. 8d). Higher intensities were observed in the areas at which S1 and S2 are located. In addition, although, the tracer intensity around points S1 and S2 seems to be approximately of the same magnitude after 10 waves (with a slight lower intensity at S1), the corresponding dissolution curves showed greater differences. Nevertheless, it has to be acknowledged that the PET is an accelerated mimic of the dissolution test, since an APS wave was occurring every 10 s compared with an APS wave every 5 min in the dissolution experiments. In addition, the drug is gradually released from the tablet resulting in a continuous "injection" in the solution making actually the dissolution experiment a repeating cycle of the PET experiment. Practically this means that a high concentration of the drug will always be observed at the beginning of the DCM tube, representing the injection point in PET experiments (Fig. 8a), and after several APSs the drug will be gradually distributed along the tube as shown in Fig. 8b–d.

The PET images represent an approximation of the distribution of the drug giving information about the zones of high and low concentrations. In particular, only a small portion of the tracer reached the very end of the tube, where the S3 is located (Fig. 8d). This explains why low release rates (e.g. 45% @ 9 h) were obtained in the dissolution profiles at point S3 in 0.25% NaCMC (w/w). In addition, radioactive tracer was mainly accumulated around point S2 whereas a slight decrease was observed at S1 (Fig. 8d). The same pattern was observed in dissolution test in which the release rate was increasing and was getting closer to that of S1 as the end of the experiment was reached.

Further increase in viscosity leads to a different profile of the distribution of the radioactive tracer. With 0.50% NaCMC (w/w) (Fig. 9) a significant amount of the tracer remained at the beginning of the tube whereas another considerable amount appeared between the points S2 and S3 after 5 (Fig. 9c) and 10 (Fig. 9d) APSs waves. However, close to S2 a slight increase in the intensity of the radiolabelled solution was observed due to the backward tailing of the radioactive tracer caused by the backflow formed as the APSs wave reached the very end of the tube. In addition, no tracer reached the very end of the tube explaining why very low release

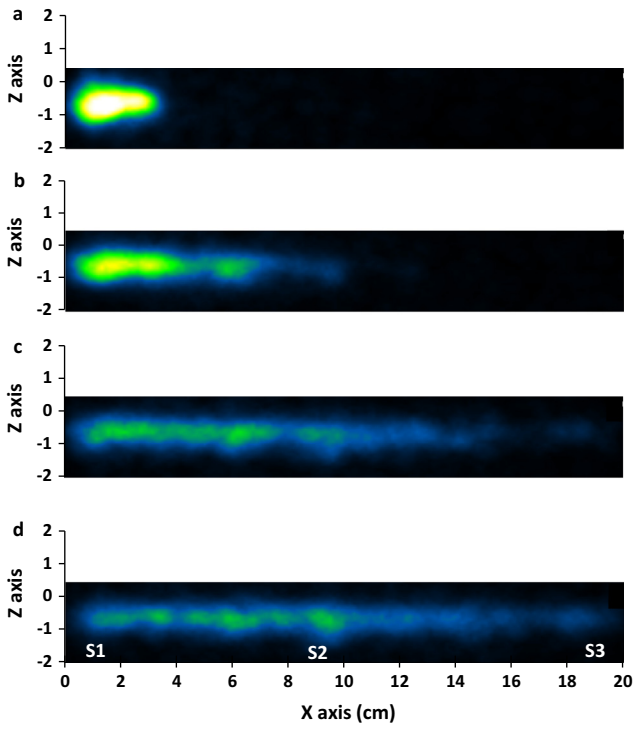


**Fig. 8.** PET images of (a) injection, (b) first wave, (c) fifth wave and (d) tenth wave using 0.25% NaCMC (w/w).

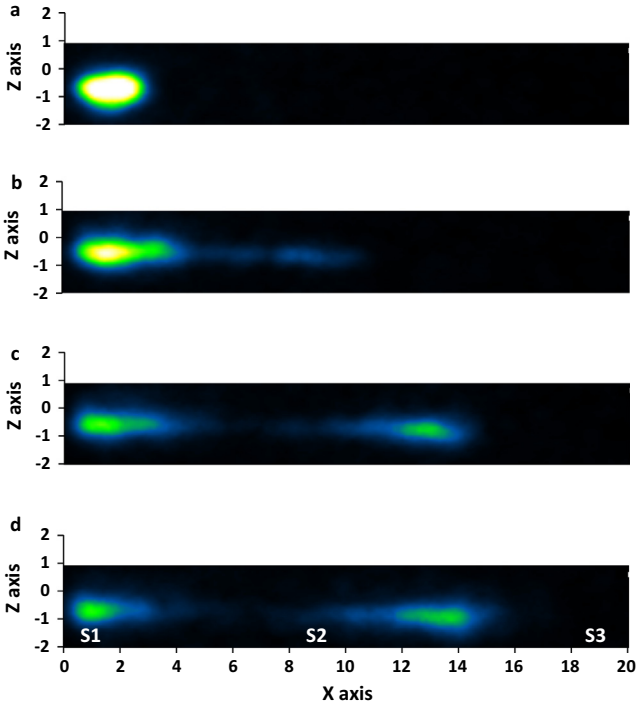


**Fig. 9.** PET images of (a) injection, (b) first wave, (c) fifth wave and (d) tenth wave using 0.50% NaCMC (w/w).

rates, almost zero per cent, were found in 0.50% NaCMC (w/w) based on the dissolution data obtained from samples collected in S3 location.

Furthermore, due to the DCM wall motion and the partial disintegration of the tablet, fragments of the dosage form were found several centimetres from the first segment of the model (Fig. 7A). Assuming that the drug will be mainly accumulated around the fragments, areas of high drug concentrations (Fig. 7B) might be differently distributed along the DCM tube with respect to the spots of high intensities of the tracer, as indicated in PET images of 0.50% NaCMC (w/w) (Fig. 9). In particular, PET experiments showed one spot close to the injection point and another one several centimetres further from the S2 (Fig. 9d). However, elongation of the first spot was observed towards the direction of the wave whereas lengthening of the second spot was appeared mainly in the opposite direction due to the backflow which is stronger as getting closer to the very end of the tube. Thus, tracers of the radioactive solution were detected close to S2. Thus, this 'to and fro' fluid motion will also affect the distribution of the drug. Hence, if the tablet or fragments are located between S1 and S2, it is likely that "elongation" of the high drug accumulation area might be occurred in both directions (Fig. 7B; first case). As a further consequence the release rates of the drug obtained from S1 to S2 will be approximately similar (Fig. 6b). In contrast, when the tablet remains in the first segment and only a small fragment is located a few centimetres further, the distribution of the drug might be looked like as in the second case (Fig. 7B; second case) and the corresponding release rates as shown in Fig. 6a.

Although PET images do not actually show the entire distribution of the drug, valuable information can be obtained about the high and low accumulation zones of the drug in viscous media. However, the protocol of the PET experiments is not far from what is applied *in vivo* during scintigraphy studies, since a watery solution is injected in human colon without knowing the actual viscosity of the colonic fluids which is presumably higher than that of the radioactive solution.

### 3.4. Comparison of the DCM with the compendial mini volume USP 2 dissolution apparatus

Table 1 presents the release rates of theophylline in different viscous media as published by Stamatopoulos et al. [36]. The release rates obtained from DCM showed higher variability between the sampling points compared to the mini volume USP 2; this is a result of the more realistic geometry and motility within the DCM. However, this means that the comparison of the two dissolution apparatuses is not straightforward due to different configuration. In DCM tube the medium fills 50% of the tube whereas the flow is induced by the wall motion as well as by the reflux of the fluid. In addition, in DCM there is a discontinuous wall motion in comparison with the continuous impeller rotation in USP 2. Furthermore, in USP 2 the tablet is normally placed within the stagnant zone below the shaft in which low velocities [36] and low shear rates [42] have been reported and which are not changing as the agitation speed is increased [42]. In contrast the dosage form faces a dynamic environment in the DCM tube in which disintegra-

**Table 1**
Comparison of the release rates of the theophylline obtained from Dynamic Colon Model (DCM) with the published data obtained from mini volume USP 2.

| Time (h) | %NaCMC (w/w) | | | |
|---|---|---|---|---|
| | 0.25% | | 0.50% | |
| | DCM[a] | Mini USP 2[b] | DCM[a] | Mini USP 2[b] |
| 2 | 3.7–30.7 | 10.0–15.0 | 0.2–29.5 | 10.0–12.0 |
| 6 | 15.0–76.6 | 30.0–40.0 | 0.5–82.4 | 30.0–50.0 |
| 8 | 34.8–85.5 | 45.0–58.0 | 3.0–76.7 | 40.0–55.0 |

[a] The low limit of the ranges corresponds to the third sampling point (S3) and the high one to the first sampling point (S1).
[b] The low values correspond to the SP1 (close to the surface of the medium) and the high to the SP2 (close to the tip) [36].

tion takes place due to the oscillation of the flexible wall. Moreover, by reproducing the architecture of the smooth muscle and the dimensions of the proximal colon, DCM provides information about the distribution of the drug with respect to the available surface area of the colonic wall. Moreover, mimicking the variability in the distribution of the drug could be useful to evaluate the variability in humans. This is not possible with the compendial dissolution methods (e.g. USP 1–4 dissolution apparatus) or with their improvements like stress test apparatus [5] or with the most advanced multi-compartmental computer controlled large intestine simulator (TIM-2, TNO) since the volume, dimensions and the geometry are not relevant to the physical organ [43].

## 4. Conclusions

A novel *in vitro* model of the human proximal colon was developed focusing mainly on the ascending colon. The proposed model can successfully reproduce the physical amplitudes within the human colon generated by the wall motion of the Dynamic Colon Model (DCM) and recorded using a solid state catheter. A direct association of the magnitude of the pressure signal with the occlusion rate of the membrane and the viscosity of the fluid was found. Thus a dosage form will experience biorelevant pressures during its passage through the DCM.

Dissolution experiments of theophylline released from $NaCMC_{(90,000)}$ based tablets were performed in different viscous media and under fixed wall motion profile similar to the main colon motility pattern recorded *in vivo* in healthy humans [22]. Thus, the disintegration of the tablet and the release of the drug took place under biorelevant conditions. However, the exact history of the pressures applied on the tablet during the repeated wave pressures needs to be investigated by tracking the position of the tablet. This will allow to evaluate whether the tablet was phasing pressures within the range measured in the centre of the contracting point or lower which probably takes place between the pockets.

The distribution of the drug was determined by collecting samples from different locations along the DCM tube and performing Positron Emission Tomography (PET). The results showed areas of high and low accumulation of the drug. Thus, using the proposed *in vitro* model it is possible to assess the behaviour not only of the dosage form but also how the drug will be distributed along the human colon, assuming that the more the surface area that the drug would be exposed the higher the possibility of being absorbed by the GI tract or the more available for local therapy. In addition, this information might allow understanding how of phenomena such as supersaturation and precipitation of the drug during the passage of the dosage form through the proximal colon.

Further work was required to examine other types of dosage forms, media volume as well as different motility patterns.

## Acknowledgements

Kostas Stamatopoulos is sponsored by an EPSRC DTG studentship at the School of Chemical Engineering, the University of Birmingham.

## Appendix A. Supplementary material

Supplementary data associated with this article can be found, in the online version, at http://dx.doi.org/10.1016/j.ejpb.2016.08.004.

## References

[1] K.H. Antonin, R. Rak, P.R. Bieck, R. Preiss, U. Schenker, J. Hastewell, R. Fox, M. Mackay, The absorption of human calcitonin from the transverse colon of man, Int. J. Pharm. 130 (1996) 33–39, http://dx.doi.org/10.1016/0378-5173(95)04248-2.

[2] H. Tozaki, J. Komoike, C. Tada, T. Maruyama, A. Terabe, T. Suzuki, A. Yamamoto, S. Muranishi, Chitosan capsules for colon-specific drug delivery: improvement of insulin absorption from the rat colon, J. Pharm. Sci. 86 (1997) 1016–1021.

[3] V. Sinha, A. Singh, R.V. Kumar, S. Singh, R. Kumria, J. Bhinge, Oral colon-specific drug delivery of protein and peptide drugs, Crit. Rev. Ther. Drug Carrier Syst. 24 (2007) 63–92.

[4] V.R. Sinha, R. Kumria, Microbially triggered drug delivery to the colon, Eur. J. Pharm. Sci. 18 (2003) 3–18, http://dx.doi.org/10.1016/S0928-0987(02)00221-X.

[5] G. Garbacz, R.-S. Wedemeyer, S. Nagel, T. Giessmann, H. Mönnikes, C.G. Wilson, W. Siegmund, W. Weitschies, Irregular absorption profiles observed from diclofenac extended release tablets can be predicted using a dissolution test apparatus that mimics in vivo physical stresses, Eur. J. Pharm. Biopharm. 70 (2008) 421–428, http://dx.doi.org/10.1016/j.ejpb.2008.05.029.

[6] G. Garbacz, S. Klein, Dissolution testing of oral modified-release dosage forms, J. Pharm. Pharmacol. 64 (2012) 944–968.

[7] N. Fotaki, A. Aivaliotis, J. Butler, J. Dressman, M. Fischbach, J. Hempenstall, S. Klein, C. Reppas, A comparative study of different release apparatus in generating in vitro-in vivo correlations for extended release formulations, Eur. J. Pharm. Biopharm. 73 (2009) 115–120.

[8] P. Spratt, C. Nicolella, D.L. Pyle, An engineering model of the human colon, Food Bioprod. Process. 83 (2005) 147–157, http://dx.doi.org/10.1205/fbp.04396.

[9] R.C. Schellekens, F.E. Stuurman, F.H. van der Weert, J.G. Kosterink, H.W. Frijlink, A novel dissolution method relevant to intestinal release behaviour and its application in the evaluation of modified release mesalazine products, Eur. J. Pharm. Sci. 30 (2007) 15–20.

[10] E. Jantratid, V. De Maio, E. Ronda, V. Mattavelli, M. Vertzoni, J.B. Dressman, Application of biorelevant dissolution tests to the prediction of in vivo performance of diclofenac sodium from an oral modified-release pellet dosage form, Eur. J. Pharm. Sci. 37 (2009) 434–441.

[11] S. Klein, The use of biorelevant dissolution media to forecast the in vivo performance of a drug, AAPS J. 12 (2010) 397–406, http://dx.doi.org/10.1208/s12248-010-9203-3.

[12] E. Jantratid, N. Janssen, H. Chokshi, K. Tang, J.B. Dressman, Designing biorelevant dissolution tests for lipid formulations: case example – lipid suspension of RZ-50, Eur. J. Pharm. Biopharm. 69 (2008) 776–785, http://dx.doi.org/10.1016/j.ejpb.2007.12.010.

[13] C. Wagner, E. Jantratid, F. Kesisoglou, M. Vertzoni, C. Reppas, J.B. Dressman, Predicting the oral absorption of a poorly soluble, poorly permeable weak base using biorelevant dissolution and transfer model tests coupled with a physiologically based pharmacokinetic model, Eur. J. Pharm. Biopharm. 82 (2012) 127–138, http://dx.doi.org/10.1016/j.ejpb.2012.05.008.

[14] U. Klančar, B. Markun, S. Baumgartner, I. Legen, A novel beads-based dissolution method for the in vitro evaluation of extended release HPMC matrix tablets and the correlation with the in vivo data, AAPS J. 15 (2013) 267–277, http://dx.doi.org/10.1208/s12248-012-9422-x.

[15] B. Abrahamsson, A. Pal, M. Sjoberg, M. Carlsson, E. Laurell, J.G. Brasseur, A novel in vitro and numerical analysis of shear-induced drug release from extended-release tablets in the fed stomach, Pharm. Res. 22 (2005) 1215–1226.

[16] E.C. Thuenemann, G. Mandalari, G.T. Rich, R.M. Faulks, Dynamic Gastric Model (DGM), in: K. Verhoeckx, P. Cotter, I. López-Expósito, C. Kleiveland, T. Lea, A. Mackie, T. Requena, D. Swiatecka, H. Wichers (Eds.), The Impact of Food Bioactives on Health: In Vitro and Ex Vivo Models, Springer International Publishing, Cham, 2015, pp. 47–59.

[17] S. Blanquet, E. Zeijdner, E. Beyssac, J.P. Meunier, S. Denis, R. Havenaar, M. Alric, A dynamic artificial gastrointestinal system for studying the behavior of orally administered drug dosage forms under various physiological conditions, Pharm. Res. 21 (2004) 585–591.

[18] W.M. Bayliss, E.H. Starling, The movements and innervation of the small intestine, J. Physiol. 24 (1899) 99–143.

[19] M.D. Sinnott, P.W. Cleary, J.W. Arkwright, P.G. Dinning, Investigating the relationships between peristaltic contraction and fluid transport in the human colon using Smoothed Particle Hydrodynamics, Comput. Biol. Med. 42 (2012) 492–503.

[20] A.E. Bharucha, S.J.H. Brookes, Neurophysiologic mechanisms of human large intestinal motility, Physiol. Gastrointest. Tract (2012) 977–1022.

[21] P. Langer, Á. Takács, Why are taeniae, haustra, and semilunar folds differentiated in the gastrointestinal tract of mammals, including man?, J Morphol. 259 (2004) 308–315, http://dx.doi.org/10.1002/jmor.10176.

[22] P.G. Dinning, L. Wiklendt, L. Maslen, I. Gibbins, V. Patton, J.W. Arkwright, D.Z. Lubowski, G. O'Grady, P.A. Bampton, S.J. Brookes, et al., Quantification of in vivo colonic motor patterns in healthy humans before and after a meal revealed by high-resolution fiber-optic manometry, Neurogastroenterol. Motil. 26 (2014) 1443–1457.

[23] P. Hiroz, V. Schlageter, J.C. Givel, P. Kucera, Colonic movements in healthy subjects as monitored by a Magnet Tracking System, Neurogastroenterol. Motil. 21 (2009) 1365–2982.

[24] S.S. Rao, B. Kuo, R.W. McCallum, W.D. Chey, J.K. DiBaise, W.L. Hasler, K.L. Koch, J.M. Lackner, C. Miller, R. Saad, et al., Investigation of colonic and whole-gut transit with wireless motility capsule and radiopaque markers in constipation, Clin. Gastroenterol. Hepatol. 7 (2009) 537–544.

[25] P.G. Dinning, M.M. Szczesniak, I.J. Cook, Proximal colonic propagating pressure waves sequences and their relationship with movements of content in the

proximal human colon, Neurogastroenterol. Motil. 20 (2008) 512–520, http://dx.doi.org/10.1111/j.1365-2982.2007.01060.x.
[26] G.I. Gabrio Bassotti, Serafina. Fiorella, Luis. Bustos-Fernandez, Claudio R. Bilder, Colonic motility in man: features in normal subjects and in patients with chronic idiopathic constipation, Am. J. Gastroenterol. 97 (1999) 1760–1770.
[27] A.E. Bharucha, High amplitude propagated contractions, Neurogastroenterol. Motil. Off. J. Eur. Gastrointest. Motil. Soc. 24 (2012) 977–982, http://dx.doi.org/10.1111/nmo.12019.
[28] J.W. Arkwright, A. Dickson, S.A. Maunder, N.G. Blenman, J. Lim, G. O'Grady, R. Archer, M. Costa, N.J. Spencer, S. Brookes, et al., The effect of luminal content and rate of occlusion on the interpretation of colonic manometry, Neurogastroenterol. Motil. 25 (2013) 10.
[29] K. Venema, The TNO in vitro model of the colon (TIM-2), in: K. Verhoeckx, P. Cotter, I. López-Expósito, C. Kleiveland, T. Lea, A. Mackie, T. Requena, D. Swiatecka, H. Wichers (Eds.), The Impact of Food Bioactives on Health: In Vitro and Ex Vivo Models, Springer International Publishing, Cham, 2015, pp. 293–304.
[30] M. Proano, M. Camilleri, S.F. Phillips, M.L. Brown, G.M. Thomforde, Transit of solids through the human colon: regional quantification in the unprepared bowel, Am. J. Physiol. 258 (1990) G856–862.
[31] C. Tannergren, A. Bergendal, H. Lennernas, B. Abrahamsson, Toward an increased understanding of the barriers to colonic drug absorption in humans: implications for early controlled release candidate assessment, Mol. Pharm. 6 (2009) 60–73.
[32] C. Schiller, C.P. Frohlich, T. Giessmann, W. Siegmund, H. Monnikes, N. Hosten, W. Weitschies, Intestinal fluid volumes and transit of dosage forms as assessed by magnetic resonance imaging, Aliment. Pharmacol. Ther. 22 (2005) 971–979.
[33] S.C. Sutton, Role of physiological intestinal water in oral absorption, AAPS J. 11 (2009) 277–285.
[34] S. Sadahiro, T. Ohmura, Y. Yamada, T. Saito, Y. Taki, Analysis of length and surface area of each segment of the large intestine according to age, sex and physique, Surg. Radiol. Anat. 14 (1992) 251–257.
[35] S. Amidon, J.E. Brown, V.S. Dave, Colon-targeted oral drug delivery systems: design trends and approaches, AAPS PharmSciTech 16 (2015) 731–741.
[36] K. Stamatopoulos, H.K. Batchelor, F. Alberini, J. Ramsay, M.J. Simmons, Understanding the impact of media viscosity on dissolution of a highly water soluble drug within a USP 2 mini vessel dissolution apparatus using an optical planar induced fluorescence (PLIF) method, Int. J. Pharm. 495 (2015) 362–373.
[37] E.L. McConnell, H.M. Fadda, A.W. Basit, Gut instincts: explorations in intestinal physiology and drug delivery, Int. J. Pharm. 364 (2008) 213–226, http://dx.doi.org/10.1016/j.ijpharm.2008.05.012.
[38] C.J. Broadbent, J. Bridgwater, D.J. Parker, S.T. Keningley, P. Knight, A phenomenological study of a batch mixer using a positron camera, Powder Technol. 76 (1993) 317–329, http://dx.doi.org/10.1016/S0032-5910(05)80013-0.
[39] P.A. Bampton, P.G. Dinning, High resolution colonic manometry–what have we learnt? – A review of the literature 2012, Curr. Gastroenterol. Rep. 15 (2013) 013–0328.
[40] G. Bassotti, G. de Roberto, D. Castellani, L. Sediari, A. Morelli, Normal aspects of colorectal motility and abnormalities in slow transit constipation, World J. Gastroenterol. 11 (2005) 2691–2696.
[41] R. Palma, N. Vidon, J.J. Bernier, Maximal capacity for fluid absorption in human bowel, Dig. Dis. Sci. 26 (1981) 929–934.
[42] G. Bai, Y. Wang, P.M. Armenante, Velocity profiles and shear strain rate variability in the USP Dissolution Testing Apparatus 2 at different impeller agitation speeds, Int. J. Pharm. 403 (2011) 1–14.
[43] S. Blanquet, S. Marol-Bonnin, E. Beyssac, D. Pompon, M. Renaud, M. Alric, The 'biodrug' concept: an innovative approach to therapy, Trends Biotechnol. 19 (2001) 393–400.